Hemolytic Effects of Water-Soluble Fullerene Derivatives

Susanna Bosi,[†] Luigi Feruglio,[†] Tatiana Da Ros,*[,†] Giampiero Spalluto,[†] Barbara Gregoretti,[‡] Michela Terdoslavich,[§] Giuliana Decorti,[‡] Sabina Passamonti,*[,§] Stefano Moro,[||] and Maurizio Prato[†]

Dipartimento di Scienze Farmaceutiche, Università di Trieste, Piazzale Europa, 1-34127 Trieste, Italy, Dipartimento di Scienze Biomediche, Università di Trieste, Via Giorgieri, 7-34127 Trieste, Italy, Dipartimento di Biochimica, Biofisica e Chimica delle Macromolecole, Università di Trieste, Via Giorgeri, -34127 Trieste, Italy, and Dipartimento di Scienze Farmaceutiche, Università di Padova, Via Marzolo, 5-35131 Padova, Italy

Received March 31, 2004

A series of water-soluble fullerene C_{60} derivatives has been investigated for their cytotoxic and hemolytic properties, with the aim to correlate structure with toxicity. We observed that cationic chains induce significant toxicity while the presence of neutral or anionic moieties did not produce any response in our model. A validation of these experimental observations has been performed by theoretical studies in which hydrophilic and hydrophobic surface areas were correlated quantitatively with hemolytic properties.

Introduction

In the past decade, [60]fullerene and its derivatives have become an attractive tool in various biological models.[1−3] It is widely accepted that this class of compounds can be active as HIV-protease inhibitors,[4−7] antibacterial,[8−11] and neuroprotective agents[12−15] and are also capable, under irradiation, to induce DNA photocleavage.[16−22] However, two major problems limit the use of C_{60} and its derivatives in biological studies: (i) the low water solubility,[23,24] (ii) the potential high toxicity.[25−27]

The first problem can be partially solved by introducing one or more solubilizing chains on the C_{60} sphere.[28−30] However while unmodified fullerene seems to be not toxic, in some cases the water-soluble derivatives proved to be quite toxic in cultured cells.

We recently synthesized a series of compounds which could potentially be used as HIV inhibitors,[31] and we also reported an example of water-soluble C_{60} derivative **1** as a neuroprotective agent, which shows high toxicity in the micromolar range.[32]

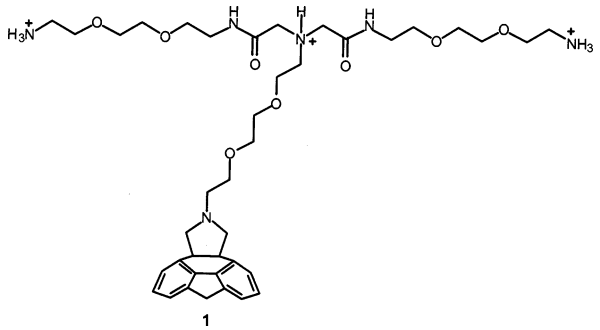

1

We hypothesized that this undesired effect could be attributed to the surfactant properties of the fullerene derivatives, generated by a simultaneous presence of hydrophobic and hydrophilic portions, which most probably induce membrane disruption.[32]

The principal aim of this work is based on the evaluation of hemolytic and cytotoxic properties of a series of bis-functionalized and water-soluble C_{60} derivatives (**2**−**10**), bearing polar chains at different positions on the spheroid. This work was also undertaken to understand which polar chains could be considered suitable for inducing water solubility in contemporary absence of toxicity. In addition, to better clarify the role of the fullerene moiety on the toxicity, compounds **11** and **12** have been synthesized as internal controls. In fact compound **11** is characterized by the presence of the same polar chain present in most derivatives used in this work, while derivative **12** can be considered a classical cationic surfactant.

To better correlate the amphiphilic properties of these derivatives and their toxicity, a quantitative theoretical study has been performed.

Results and Discussion

Derivatives **2**−**10** (Figure 1) have been prepared according to a previous report,[28] and their purity was checked by electrospray mass spectrometry (ESMS) and reverse-phase HPLC coupled with a diode array detector.[28]

The reference compounds **11** and **12** have been easily prepared by standard procedures.[11,33] Before performing the biological assays, the solubility of all the fullerene compounds in water and in phosphate buffer solution (PBS, pH 7.4) was determined by UV spectroscopy. Known amounts of all compounds were dissolved in water and/or PBS solutions to prepare the relative standard solutions. A linear calibration line was obtained. Saturated solutions of all compounds were then prepared and centrifuged to obtain clear solutions. After dilution, the solubility values were determined by interpolation using the calibration curve.[28] (Table 1)

As clearly indicated, all the compounds displayed a good solubility ranging from 10^{-2} to 10^{-4} M, which could be considered optimal for the biological screening.

* To whom correspondence should be addressed. T.D.R.: Tel. +39 040 558 3110. Fax +39 040 52572. E-mail: daros@units.it. S.P.: Tel.: +39 040 558 3681. Fax: +39 040 558 3691. E-mail: passamonti@bbcm.univ.trieste.it.

[†] Dipartimento di Scienze Farmaceutiche, Università di Trieste.

[‡] Dipartimento di Scienze Biomediche, Università di Trieste.

[§] Dipartimento di Biochimica, Biofisica e Chimica delle Macromolecole, Università di Trieste.

[||] Università di Padova.

10.1021/jm0497489 CCC: $27.50
Published on Web 12/02/2004

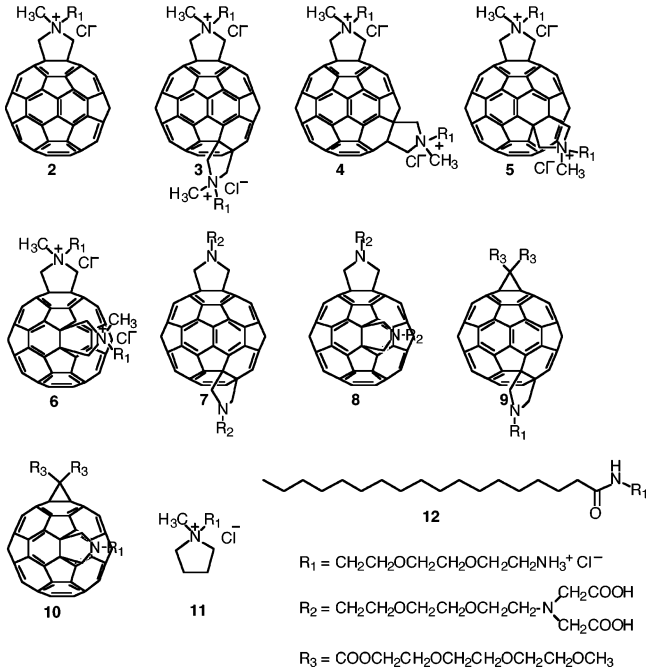

Figure 1. Structures of compounds **2**−**12**.

Table 1. Solubility of Derivative **2**−**10** in Water and in PBS

compound	water (M)	PBS (M)
2	1×10^{-4}	–
3−**6**	2×10^{-2}	3×10^{-2}
7, **8**	3.3×10^{-4}	1×10^{-2}
9, **10**	2×10^{-2}	1.2×10^{-4}

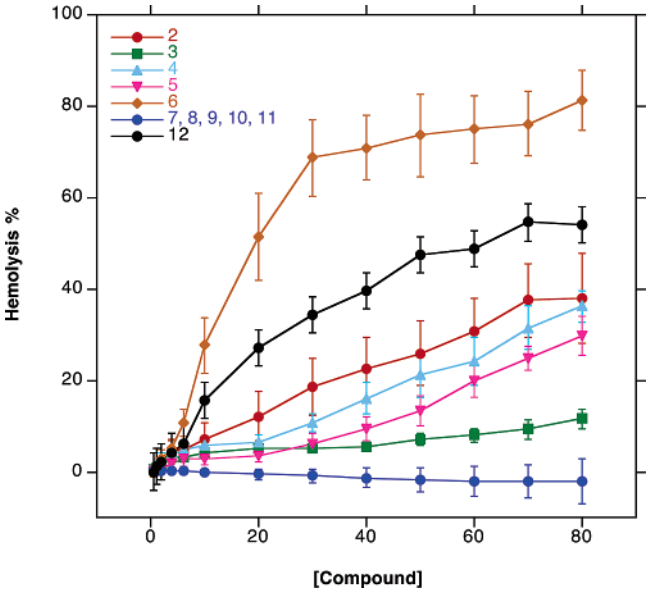

Figure 2. Hemolysis percentage induced by compounds **2**−**12**. Quadruplicated values are reported as absolute percent of hemolysis ± standard error of the mean (SEM).

The first assay was based on the evaluation of hemolytic properties of derivatives **2**−**12** in human red blood cells (Figure 2). To examine the interaction of these molecules with cells, we first tested their effect on human red blood cells (RBC), i.e., their hemolytic activity, and afterward their cytotoxic effects on three different cell lines. For the evaluation of the hemolytic activity all the compounds were dissolved at different concentrations in a saline-buffered solution at pH 7.4.

Table 2. Cytotoxicity of Compounds **3**−**12** on Hep-G2, LLC-PK$_1$, and MCF-7 Cell Lines

compd	Hep-G2 (LD_{50}, μM)	LLC-PK$_1$ (LD_{50}, μM)	MCF-7 (LD_{50}, μM)
3	20	<1	20
4	15	<1	10
5	8	<1	20
6	50	<1	15
7	>80	>80	>80
8	>80	>80	>80
9	>80	>80	>80
10	>80	>80	>80
11	>80	>80	>80
12	>80	>80	>80

These solutions were incubated with a suspension of RBC at 37 °C for 30 min. After centrifugation, the supernatant was analyzed by UV spectroscopy ($\lambda = 415$ nm), to detect hemoglobin, that is spread into the solution in case of cell disruption.

As depicted in Figure 2, derivatives **2**−**12** showed significant differences in hemolytic properties. A careful examination of data clearly indicate that bis-functionalized chains bearing carboxylic functions or only one cationic chain (**7**−**10**), independently from their relative positions, do not show any hemolytic properties up to a concentration of 80 μM. In contrast, compounds with two cationic chains (**3**−**6**) proved to be remarkably hemolytic at concentrations ranging 20−60 μM (about 40−50% of hemolysis).

In this latter case the position of the substituents on the C_{60} spheroid seems to confer a great influence on hemolytic potency. In fact, while bis-functionalized derivatives **6** (equatorial) resulted to be highly hemolytic (50% at 20 μM), the other isomers were much less efficient at the same concentration (5−10% of hemolysis).

These results are in good agreement with the hypothesis based on the surfactant properties of these derivatives. In further support, reference compound **11** resulted to be completely inactive, whereas derivative **12** proved to be quite hemolytic (30% at 20 μM).

To further validate these results for all bis-adducts **3**−**12**, the cytotoxicity on three different cell lines (human breast cancer cell line MCF7, Hep-G2 cells from rat liver and pig renal proximal tubular cell lines LLC-PK$_1$) has been tested as summarized in Table 2. Compounds were incubated with cells on multiwell plates for 30 min, then they were removed, and MTT [3-(4,5-dimethyl-2-thiazolyl)-2,5-diphenyl-2*H*-tetrazolium bromide] was added. As the result of the mitochondrial dehydrogenases activity, this dye is transformed from a pale yellow form to a strong violet derivative that absorbs at 540 nm. Derivative **2** has not been tested due to its low solubility in the media necessary to determine cytotoxicity because the high salt concentration induces precipitation of this compound.

As clearly indicated, all the fullerene derivatives possessing significant hemolytic properties (**3**−**6**) were also cytotoxic in the μM range with different degree of potency, depending on the type of substitution and the cell culture, while derivatives inactive in the hemolytic assay (**7**−**11**) did not display any cytotoxicity at concentration <80 μM.

Only the reference compound **12** behaves differently, showing hemolytic properties but being inactive in the cytotoxicity test. A possible explanation of this discrep-

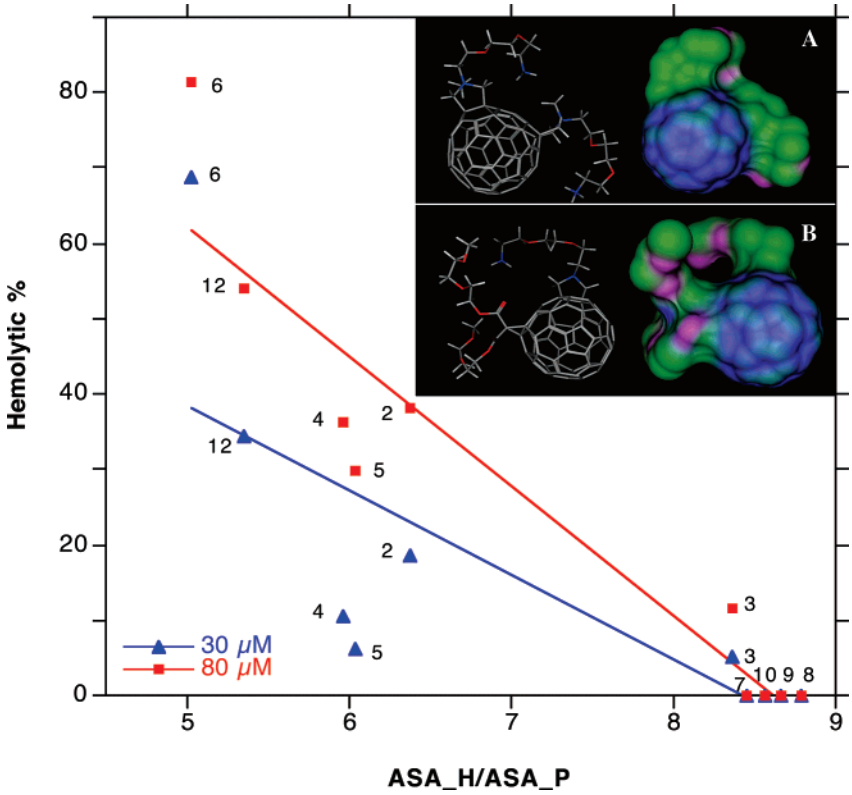

Figure 3. Ratio between ASA_H and ASA_P plots against the hemolytic activity measured at 80 μM (red square) and at 30 μM (blue triangle) concentration of each fulleropyrrolidine derivatives. The 3D structures and the hydrophobicity/hydrophilicity surfaces of compound **6** (the most hemolytic) and compound **10** (the less hemolytic) are presented in panel A and B, respectively.

ancy could be that for fullerene derivatives, other mechanisms (different from membrane cell disruption) may be involved in cytotoxicity. In fact, in the comparison of cytotoxic and hemolytic values, it is evident that cytotoxicity is significant at concentrations ranging 1−50 μM, clearly lower than concentrations at which the hemolytic process is meaningful.

Several proposed mechanisms can induce the hemolysis phenomena: drug−membrane adsorption, drug-depending antibody, autoimmune induction mechanism, and nonimmunologic drug-induced hemolysis. As already demonstrated, the primary interaction between the drug and the red cell surface is the critical step in several of the above-mentioned mechanisms. A major source of variation on drug−membrane interaction is due to balance between hydrophobicity and hydrophilicity properties of the drug. To explore the potential mechanism/s of the observed drug-induced hemolysis activity of these derivatives, a preliminary molecular modeling study has been performed.

Primarily, we exhaustively explored the conformational space of all new fulleropyrrolidine derivatives (**2**−**10**) using a stochastic conformational search method, and the GB/SA treatment as implicit solvent electrostatic correction on the MMFF94 force field (see the Experimental Section for details). We have also analyzed derivative **12** as reference compound. All fulleropyrrolidine derivatives (**2**−**10**) were edited to fix the ionization status of all amine and carboxylic groups in a corresponding reasonable solvated state. For the most stable conformer of each compound (**2**−**10**), the total hydrophobic surface area (ASA_H) and the total hydrophilic surface area (ASA_P) have been calculated. The molecular descriptors have been collected in Table 3.

Table 3. Calculated ASA_H and ASA_P Molecular Descriptors

compd	hemolytic activity (%)[a]	hemolytic activity (%)[b]	ASA_H (Å^2)[c]	ASA_P (Å^2)[d]	ASA_H/ ASA_P
2	19	38	704.21	110.43	6.37
3	5	12	911.80	109.018	8.36
4	11	36	912.84	153.027	5.96
5	6	30	871.28	144.11	6.04
6	69	81	769.36	152.97	5.02
7	0	0	1168.79	138.20	8.45
8	0	0	1450.22	164.90	8.79
9	0	0	1162.43	134.22	8.66
10	0	0	1107.77	129.40	8.56
12	34	53	582.68	108.81	5.35

[a] Hemolytic activity calculated at 30 μM of each derivative. [b] Hemolytic activity calculated at 80 μM of each derivative. [c] Total hydrophobic surface area in Å^2. [d] Total hydrophilic surface area in Å^2.

The ratio between ASA_H and ASA_P has been plotted against the hemolytic activity measured at 30 and 80 μM concentrations of each fulleropyrrolidine derivatives. Interestingly, a linear correlation plot has been obtained in both cases (30 μM, $r = 0.779$; 80 μM, $r = 0.944$) as shown in Figure 3. Even if the coefficients do not indicate a really strong correlation between hydrophilic/hydrophobic area ratio and hemolytic action, these preliminary unexpected indications are a very promising starting point for further detailed studies.

Conclusions

This preliminary study highlights a correlation between the ASA_H/ASA_P ratio and the corresponding hemolytic activities. Derivatives with relatively high ASA_H/ASA_P ratio seem to be better tolerated by red cells. In particular, polycationic fulleropyrrolidine derivatives (**2**−**6**) seem to present the crucial chemical

requirements to promote hemolytic activity. Further investigations are necessary to definitively confirm and, consequently, better clarify the pharmacological reason/s of this interesting but still preliminary computational result.

Experimental Section

Chemistry. The syntheses of fullerene derivatives **2**−**10** have been performed as previously reported.[28] **Synthesis of 11.** To a solution of 700 mg (2.82 mmol) of *N-tert*-butoxycarbonyl-2,2′-ethylenedioxybis(ethylamine)[34] and 200 mg (1.45 mmol) of K_2CO_3 in 100 mL of ethanol were slowly added 350 μL (2.82 mmol) of 1,4-dibromobutane. The mixture was stirred at 60 °C for 24 h, and then the product was purified by chromatography on alumina (ethyl acetate). $C_{15}H_{30}N_2O_4$ (MW 302.4) 380 mg, 1.26 mmol, yield 44%. ^{1}H NMR ($CDCl_3$, 200 MHz) δ 3.63−3.47 (m, 8H), 3.12 (t, J = 10.0 Hz, 2H), 2.25 (t, J = 6.0 Hz, 4H), 1.60 (m, 4H), 1.49 (s, 9H). ES-MS: *m/z* 302 (M^+). The pyrrolidine (100 mg, 0.33 mmol) was dissolved in dichloromethane (3 mL) and added by 3 mL of methyl iodide. The mixture was stirred at 80 °C in a closed vial for 24 h, the solvent and the CH_3I were removed by evaporation, and the residue was washed with toluene. $C_{16}H_{33}IN_2O_4$ (MW 444.3) 145 mg, 0.33 mmol, yield 98%. ES-MS: *m/z* 317 (M^+). HCl_g was bubbled for 5 min into a solution of methylated pyrrolidine (100 mg, 0.22 mmol) in dichloromethane (20 mL) at 0 °C. Then the mixture was stirred at rt for 2 h, the solvent was removed by evaporation, and the pure product was washed by toluene. $C_{11}ClH_{26}IN_2O_2$ (MW 380.7) 80 mg, 0.21 mmol, yield 98%. ES-MS: *m/z* 218 (M^+).

Synthesis of 12. To a solution of stearic acid (1.1 g, 3.9 mmol) in 50 mL of anhydrous dichloromethane were added 400 mg (3.9 mmol) of DCC and 50 mg of DMAP. The mixture was stirred at rt for 20 min, and then a solution of *N-tert*-butoxycarbonyl-2,2′-ethylenedioxybis(ethylamine) (960 mg, 3.9 mmol) in anhydrous dichloromethane (10 mL) was slowly added. The solution was stirred at rt overnight, and then the organic phase was washed with water and dried with anhydrous Na_2SO_4. The pure product was recovered after evaporation of the solvent and chromatography on silica gel (ethyl acetate/petroleum ether 1/1). $C_{29}H_{58}N_2O_5$ (MW 514.8) 500 mg, 1.0 mmol, yield 25%. ^{1}H NMR ($CDCl_3$, 200 MHz) δ 6.02 (bs, 1H), 5.00 (bs, 1H), 3.67−3.48 (m, 8H), 3.48−3.37 (m, 2H), 3.37−3.20 (t, J = 4.0 Hz, 2H), 2.15 (t, J = 6.0 Hz, 2H), 1.43 (s, 9H), 1.23 (m, 30H), 0.85 (m, 3H). ES-MS: *m/z* 514 (M^+). The amide (360 mg, 0.7 mmol) was dissolved in 100 mL of dichloromethane and 10 mL of TFA, and the mixture was stirred at rt overnight. The solvent and the TFA were removed by evaporation and the product was washed with toluene. $C_{26}H_{51}F_3N_2O_5$ (MW 528.7) 366 mg, 0.7 mmol, yield 99%. ES-MS: *m/z* 415 (M^+).

Biology. All solutions were prepared with MilliQ water. **Hemolysis Assay.** Solution A. Sodium phosphate-buffered solution: NaH_2PO_4−H_2O 0.004 M; Na_2HPO_4 0.006 M; NaCl 0.139 M; pH 7.4. Solution B (anticoagulant solution): Sodium citrate tribasic dihydrate 0.075 M; citric acid monohydrate 0.038 M; glucose monohydrate 0.124 M. The solution was sterilized by filtration on membrane filters (Ø = 0.22 μm). Blood was collected by venipuncture and added with 0.1 volume of solution B in 50 mL tubes. Blood was collected by venipuncture in a 50 mL vial, added with 10% ACD (anticoagulant-citrate-dextrose solution) and centrifuged for 10 min at 500*g*. The supernatant was then carefully decanted, and the pellet was washed three times by suspending it in four volumes of ice-cold solution A and discarding it after centrifugation as above. The hemolysis tests were prepared in 1.5 mL tubes, where 0.9 mL of fullerene dissolved in solution A was added and incubated at 37 °C for 5 min. Then, 0.015 mL of a 20% (v/v) suspension of RBC was added. Afer 30 min, the incubation was stopped by adding 0.5 mL of ice-cold solution A. The tubes were centrifuged at 12 000*g* for 5 min, and the supernatants were analyzed at λ = 415 nm. Since all the fullerene derivatives absorb at λ = 415 nm, corresponding fullerene solutions without RBC were prepared and used as blanks. The data obtained were related to the value of total hemolysis, obtained by incubating 0.015 mL of a 20% (v/v) suspension of RBC in 0.9 mL of solution A containing 0.1% (v/v) Triton X-100 for 30 min at 37 °C. These reference samples were centrifuged and analyzed as specified above, after appropriate dilution.

Cytotoxicity on Cell Coltures. Cells from exponentially growing cultures were harvested and dispensed within 96-well culture plates (Corning Incorporated) in 200 μL of medium at the concentration of 10^5 cells/well. After 30 min of incubation at 37 °C, fullerene derivatives were added at increasing concentrations, and the incubation was continued for predetermined times (30 min, 24, 48, and 72 h). MTT (20 μL of solution 5 mg/mL in D-PBS, Aldrich) was added to each well. After 4 h incubation at 37 °C, supernatants were removed by careful aspiration and the formazane salt was solubilized with 200 μL of DMSO (Carlo Erba Italia). Optical density of each well was measured using an Automated Microplate Reader (Bio-Tek Instruments) at λ = 540 nm (reference λ = 630 nm). The percentage of living cells is expressed as the percent ratio of optical density in the treated over the untreated samples, and eight independent values were averaged for each treatment. The IC_{50} was defined as the concentration of the substance required to reduce the optical density in each test to 50% of control.

Computational Methodologies. All molecular modeling studies were carried out on a six-CPU (PIV 2.0−3.0 GHZ) linux cluster running under openMosix architecture.[35]

Functionalized fulleropyrrolidine structures were built up using Molecular Operating Environment (MOE, 2002.03) modeling package[36] and fully optimized without geometry constraints using RHF/AM1 semiempirical calculations. Atomic charges were calculated by fitting to electrostatic potential maps. The software package SpartanO2 was utilized for all quantum mechanical calculations.[37]

To explore the conformational space of functionalized fulleropyrrolidine moiety, we performed an exhaustive conformational analyis by using the Stochastic Conformational Search algorithm (SCS) implemented by MOE.[38] SCS method generates conformations by randomly sampling local minima of the potential energy surface. This method generates new molecular conformations by randomly perturbing the position of each coordinate of each atom in the molecule by some small amount, typically less than 2 Å, followed by energy minimization. This minimization is intended to relieve bad nonbonded contacts. During SCS run, we collected 55 conformations sorted by their conformational energies. The most stable conformer has been optimized using MMFF94 force field[39−45] implemented by MOE until the rms value of the conjugate gradient was <0.01 kcal/mol/Å. To model the effects of solvent more directly, a set of electrostatic interaction corrections are used. MOE suite implemented a modified version of GB/SA contact function described by Still and coauthors.[46] These terms model the electrostatic contribution to the free energy of solvation in a continuum solvent model. Molecular descriptors, such as hydrophobic and hydrophilic surfaces, have been calculated by using MOE-QSAR module.

Acknowledgment. This work was supported by the University of Trieste (Fondi 60%), by MIUR (PRIN 2002, prot. n. 2002032171). The molecular modeling work coordinated by S. Moro has been carried out with financial supports of Associazione Italiana per la Ricerca sul Cancro (AIRC), Milan, and the Italian Ministry for University and Research (MIUR), Rome, Italy. S. Moro is also grateful to Chemical Computing Group for the scientific and technical collaboration.

References

(1) Bosi, S.; Da Ros, T.; Spalluto, G.; Prato, M. Fullerene derivatives: an attractive tool for biological application. *Eur. J. Med. Chem.* **2003**, *38*, 913−923.
(2) Nakamura, E.; Isobe, H. Functionalized fullerenes in water. The first 10 years of their chemistry, biology, and nanoscience. *Acc. Chem. Res.* **2003**, *36*, 807−815.

(3) Da Ros, T.; Prato, M. Medicinal Chemistry with Fullerenes and Fullerene Derivatives. *Chem. Commun.* **1999**, 663−669.
(4) Schuster, D. I.; Wilson, L. J.; Kirschner, A. N.; Schinazi, R. F.; Schlueter-Wirtz, S.; Tharnish, P.; Barnett, T.; Ermolieff, J.; Tang, J.; Brettreich, M.; Hirsch, A. Evaluation of the anti-HIV potency of a water-soluble dendrimeric fullerene. In *Fullerene 2000—Functionalized Fullerenes*; Martin, N., Maggini, M., Guldi, D. M., Eds.; The Electrochemical Society, Inc.: Pennington, NJ, 2000; Vol. 9, pp 267−270.
(5) Friedman, S. H.; Ganapathi, P. S.; Rubin, Y.; Kenyon, G. L. Optimizing the binding of fullerene inhibitors of the HIV-1 protease through predicted increases in hydrophobic desolvation. *J. Med. Chem.* **1998**, *41*, 2424−2429.
(6) Friedman, S. H.; DeCamp, D. L.; Sijbesma, R. P.; Srdanov, G.; Wudl, F.; Kenyon, G. Inhibition of the HIV-1 Protease by Fullerene Derivatives: Model Building Studies and Experimental Verification. L. *J. Am. Chem. Soc.* **1993**, *115*, 6506−6509.
(7) Sijbesma, R.; Srdanov, G.; Wudl, F.; Castoro, J. A.; Wilkins, C.; Friedman, S. H.; DeCamp, D. L.; Kenyon, G. L. Synthesis of a fullerene derivative for the inhibition of HIV enzymes. *J. Am. Chem. Soc.* **1993**, *115*, 6510−6512.
(8) Mashino, T.; Nishikawa, D.; Takahashi, K.; Usui, N.; Yamori, T.; Seki, M.; Endo, T.; Mochizuki, M. Antibacterial and antiproliferative activity of cationic fullerene derivatives. *Bioorg. Med. Chem. Lett.* **2003**, *13*, 4395−7.
(9) Tsao, N.; Luh, T.; Chou, C.; Chang, T.; Wu, J.; Liu, C.; Lei, H. In vitro action of carboxyfullerene. *J. Antimicrob. Chemother.* **2002**, *49*, 641−649.
(10) Tsao, N.; Luh, T.; Chou, C.; Wu, J.; Lin, Y.; Lei, H. Inhibition of group A streptococcus infection by carboxyfullerene. *Antimicrob. Agents Chemother*. **2001**, *45*, 1788−93.
(11) Bosi, S.; Da Ros, T.; Castellano, S.; Banfi, E.; Prato, M. Antimycobacterial activity of ionic fullerene derivatives. *Bioorg. Med. Chem. Lett.* **2000**, *10*, 1043−1045.
(12) Huang, S. S.; Tsai, S. K.; Chin, C. L.; Chiang, L.-Y.; Hsieh, H. M.; Teng, C. M.; Tsai, M. C. Neuroprotective effect of hexasulfobutylated C_{60} on rats subjected to focal cerebral ischemia. *Free Rad. Biol. Med.* **2001**, *30*, 643−649.
(13) Dugan, L. L.; Lovett, E.; Cuddihy, S.; Ma, B.-W.; Lin, T.-S.; Choi, D. W. Carboxyfullerenes as neuroprotective antioxidants. In *Fullerenes: Chemistry, Physics, and Technology*; Kadish, K. M., Ruoff, R. S., Eds.; John Wiley & Sons: New York, 2000; pp 467−479.
(14) Lin, A.; Chyi, B.; Wang, S.; Yu, H.; Kanakamma, P.; Luh, T.-Y.; Chou, C.; Ho, L. Carboxyfullerene prevents iron-induced oxidative stress in rat brain. *J. Neurochem.* **1999**, *72*, 1634−1640.
(15) Dugan, L.; Gabrielsen, J.; Yu, S.; Lin, T.; Choi, D. Buckminsterfullerenol free radical scavengers reduce excitotoxic and apoptotic death of cultured cortical neurons. *Neurobiol. Dis.* **1996**, *3*, 129−135.
(16) Da Ros, T.; Bergamin, M.; Vázquez, E.; Spalluto, G.; Baiti, B.; Moro, S.; Boutorine, A.; Prato, M. Synthesis and Molecular Modeling Studies of Fullerene-Trimethoxyindole-Oligonucleotide Conjugates as Possible Probes for Studying Photochemical Reactions in DNA Triple Helices. *Eur. J. Org. Chem.* **2002**, 405−413.
(17) Takenaka, S.; Yamashita, K.; Takagi, M.; Hatta, T.; Tsuge, O. Photoinduced DNA cleavage by water-soluble cationic fullerene derivatives. *Chem. Lett.* **1999**, 321−322.
(18) Ikeda, A.; Hatano, T.; Kawaguchi, M.; Suenaga, H.; Shinkai, S. Water-soluble [60]fullerene-cationic homooxacalix[3]arene complex which is applicable to the photocleavage of DNA. *Chem. Commun.* **1999**, *15*, 1403−1404.
(19) Bernstein, R.; Prat, F.; Foote, C. S. On the mechanism of DNA cleavage by fullerene investigated in model systems: electron transfer from guanosine and 8-oxo-guanosine derivatives to C_{60}. *J. Am. Chem. Soc.* **1999**, *121*, 464−465.
(20) Nakamura, E.; Tokuyama, H.; Yamago, S.; Shiraki, T.; Sugiura, Y. Biological activity of water-soluble fullerenes. Structural dependence of DNA cleavage, cytotoxicity, and enzyme inhibitory activities including HIV−Protease inhibition. *Bull. Chem. Soc. Jpn.* **1996**, *69*, 2143−2151.
(21) Boutorine, A. S.; Tokuyama, H.; Takasugi, M.; Isobe, H.; Nakamura, E.; Hélène, C. Fullerene-oligonucleotide conjugates: Photoinduced sequence-specific DNA cleavage. *Angew. Chem., Int. Ed. Engl.* **1994**, *33*, 2462−2465.
(22) Tokuyama, H.; Yamago, S.; Nakamura, E.; Shiraki, T.; Sugiura, Y. Photoinduced biochemical activity of fullerene carboxylic acid. *J. Am. Chem. Soc.* **1993**, *115*, 7918−7919.
(23) Ruoff, R. S.; Tse, D. S.; Malhotra, R.; Lorents, D. C. Solubility of C_{60} in a variety of solvents. *J. Phys. Chem.* **1993**, *97*, 3379−3383.
(24) Sivaraman, N.; Dhamodaran, R.; Kaliappan, I.; Srinivasan, G.; Vasudeva Rao, P. R.; Mathews, C. K. Solubility of C_{60} in organic solvents. *J. Org. Chem.* **1992**, *57*, 6077−6079.
(25) Yang, X.; Fan, C.; Zhu, H. Photoinduced cytotoxicity of malonic acid [C_{60}]fullerene derivatives and its mechanism. *Toxicol. In Vitro* **2002**, *16*, 41−46.
(26) Chen, H.; Yu, C.; Ueng, T.; Chen, S.; Chen, B.; Huang, K.; Chiang, L. Acute and subacute toxicity study of water-soluble polyalkylsulfonated C_{60} in rats. *Toxicol. Pathol*. **1998**, *26*, 143−151.
(27) Yamago, S.; Tokuyama, H.; Nakamura, E.; Kikuchi, K.; Kananishi, S.; Sueki, K.; Nakahara, H.; Enomoto, S.; Ambe, F. In vivo biological behavior of a water-miscible fullerene −C^{14} labeling, absorption, distribution, excretion and acute toxicity. *Chem. Biol.* **1995**, *2*, 385−389.
(28) Bosi, S.; Feruglio, L.; Milic, D.; Prato, M. Synthesis and Water Solubility of Novel Fullerene Bisadduct Derivatives. *Eur. J. Org. Chem.* **2003**, 4741−4747.
(29) Filippone, S.; Heimann, F.; Rassat, A. A highly water-soluble 2:1 beta-cyclodextrin-fullerene conjugate. *Chem. Commun.* **2002**, 1508−1509.
(30) Brettreich, M.; Hirsch, A. A highly water-soluble dendro[60]-fullerene. *Tetrahedron Lett.* **1998**, *39*, 2731−2734.
(31) Bosi, S.; Da Ros, T.; Spalluto, G.; Balzarini, J.; Prato, M. Synthesis and anti-HIV properties of new water-soluble bisfunctionalized [60]fullerene derivatives. *Bioorg. Med. Chem. Lett.* **2003**, *13*, 4437−4440.
(32) Cusan, C.; Da Ros, T.; Spalluto, G.; Foley, S.; Janot, J.-M.; Seta, P.; Larroque, C.; Tomasini, M. C.; Antonelli, T.; Ferraro, L.; Prato, M. A new multi-charged C_{60} derivative: synthesis and biological properties. *Eur. J. Org. Chem.* **2002**, *17*, 2928−2934.
(33) Reddy, K. S.; Sola, L.; Moyano, A.; Pericas, M. A.; Riera, A. Highly efficient synthesis of enantiomerically pure (s)-2-amino-1,2,2-triphenylethanol. Development of a new family of ligands for the highly enantioselective catalytic ethylation of aldehydes. *J. Org. Chem.* **1999**, *64*, 3969−3974.
(34) Beer, P. D.; Cadman, J.; Lloris, J. M.; Martinez-Manez, R.; Soto, J.; Pardo, T.; Marcos, D. Anion interaction with ferrocene-functionalized cyclic and open-chain polyaza and aza-oxa cycloalkanes. *J. Chem. Soc., Dalton Trans.* **2000**, 1805−1812.
(35) OpenMosix, http://www.openMosix.org.
(36) Molecular Operating Environment (MOE 2003.02), C. C. G., Inc, 1255 University St., Suite 1600, Montreal, Quebec, Canada, H3B 3X3.
(37) Spartan O2, W. I., 18401 Von Karman Ave., Irvine, CA 92612.
(38) Ferguson, D. M.; Raber, D. J. A new approach to probing conformational space with molecular mechanics: random incremental pulse search. *J. Am. Chem. Soc.* **1989**, *111*, 4371−4378.
(39) Halgren, T. A. MMFF 4. Conformational energies and geometries for MMFF94. *J. Comput. Chem.* **1996**, *17*, 587−615.
(40) Halgren, T. A. MMFF 3. Molecular geometries and vibrational frequencies for MMFF94. *J. Comput. Chem.* **1996**, *17*, 553−586.
(41) Halgren, T. A. MMFF 2. MMFF94 van der Waals and electrostatic parameters for intermolecular interactions. *J. Comput. Chem.* **1996**, *17*, 520−552.
(42) Halgren, T. A. MMFF 1. Basis, form, scope, parametrization, and performance of MMFF94. *J. Comput. Chem.* **1996**, *17*, 490−519.
(43) Halgren, T. A. MMFF 7. Characterization of MMFF94, MMFF94s, and other widely available force fields for conformational energies and for intermolecular-interaction energies and geometries. *J. Comput Chem.* **1999**, *20*, 730−748.
(44) Halgren, T. A. MMFF 6. MMFF94s Option for energy minimization studies. *J. Comput Chem.* **1999**, *20*, 720−729.
(45) Halgren, T. A.; Nachbar, R. MMFF 5. Extension of MMFF94 Using experimental data, additional computational data, and empirical rules. *J. Comput. Chem.* **1996**, *17*, 616−641.
(46) Qiu, D.; Shenkin, S.; Hollinger, F. P.; Still, W. C. The GB/SA Continuum Model for Solvation. A fast analytical method for the calculation of approximate Born radii. *J. Phys. Chem.* **1997**, *101*, 3005−3017.

JM0497489